



High mass exclusive dijet production in the D0 experiment

The D0 Collaboration

(Dated: March 12, 2010)

Evidence is presented for diffractive exclusive dijet production with an invariant mass greater than 100 GeV in Run II of the Fermilab Tevatron Collider in the D0 experiment. A discriminant variable based on calorimeter information is used to demonstrate a significant excess of events with very little energy outside the dijet system. The probability for the observed excess to be explained by other dijet production processes is 2×10^{-5} , corresponding to a 4.1 standard deviation significance.

Preliminary Results for Winter 2010 Conferences

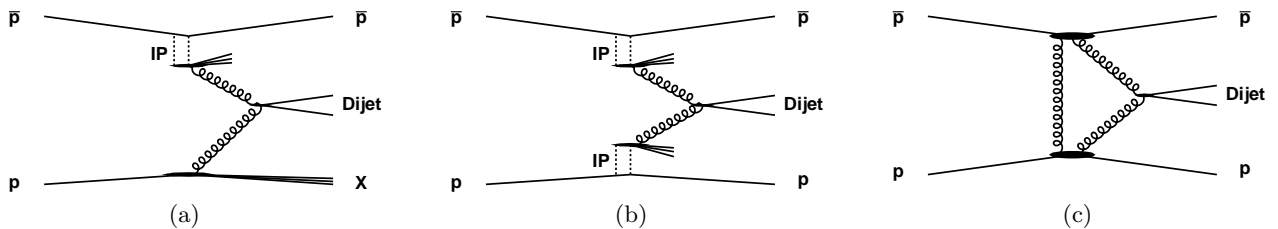


FIG. 1: Hard diffraction production of central dijet events: (a) single diffraction, in which only either the proton or the antiproton is diffracted by a Pomeron (IP) exchange, while the other breaks up; (b) inclusive double Pomeron, where proton and antiproton remain intact, and additional QCD radiation can be observed from Pomeron remnants; and (c) exclusive diffractive production where both protons remain intact and only the dijet is produced in the central region.

Hard diffraction was first observed experimentally twenty years ago in the UA8 experiment at CERN and has been studied extensively in many experiments such as H1 and ZEUS at HERA and D0 and CDF at the Tevatron [1]. At hadron colliders, hard diffractive events are identified by the presence of a gap devoid of any activity in the forward region of the detector [2] and/or by tagging intact beam hadrons in the final state. Hard diffractive events are generally described by the exchange of a colorless object, referred to as the Pomeron. Diffractively produced objects such as dijets, diphotons, χ_C charmonium, and others can be observed in the detector together with the Pomeron remnants. A recently introduced subset of hard diffractive events called exclusive [3, 4] is defined such that all the available energy is used to produce the diffractive object or, in other words, no energy is lost to Pomeron remnants. In this note, we search for this type of events in the high dijet invariant mass region.

Exclusive diffractive production (EDP) of a final state X , $p\bar{p} \rightarrow p + X + \bar{p}$, has been recently proposed as a search channel for new physics and the Higgs boson at the Large Hadron Collider (LHC) [4]. In this process, kinematical properties such as the mass of the object X can also be computed with high precision by measuring only the energy loss of the outgoing protons in the final state. Even if the cross section is too low to produce Higgs bosons in exclusive diffraction at the Tevatron (a cross section of about 0.2 fb is predicted for a Higgs mass of 120 GeV), it is important to check if the EDP class of events exists in this kinematical region. The CDF collaboration recently reported the existence of exclusive diffractive events in the dijet, dielectron, diphoton and charmonium channels [5]. These results support the existence of EDP, but are mainly restricted to lower mass objects (typically less than 100 GeV), while at the LHC, new physics is expected to appear at higher masses. In this note, we report evidence for exclusive diffractive dijet events with invariant mass greater than 100 GeV in data collected with the D0 experiment.

To search for exclusive dijet production, we consider three different classes of hard diffractive production in addition to non-diffractive production: single diffractive (SD) dijet production (Fig. 1 (a)), inclusive diffractive production through double Pomeron exchange (IDP) (Fig. 1 (b)), and exclusive diffractive dijet production (Fig. 1 (c)). In SD, one of the beam hadrons remains intact while the other breaks up. In IDP, both beam hadrons are intact after the collision. The partonic structure of the Pomeron is taken from recent HERA measurements [6] and used to compute the diffractive jet production cross section at the Tevatron. An additional gap survival probability [7] multiplicative factor of 0.1 is introduced to account for soft production of particles from the underlying proton-antiproton event that populate the rapidity gaps [1].

In EDP events, there is no QCD radiation and therefore no Pomeron remnants, and the total energy loss of the incoming hadrons is used to produce the central object. The background in the search for EDP is mainly due to the tails of the multiplicity or energy distributions for small fractions of SD, IDP and non-diffractive (NDF) QCD events. NDF background events are simulated using the PYTHIA [8] Monte Carlo (MC) generator and the diffractive (SD and IDP) backgrounds are determined using the POMWIG [9] and FPMC [10] generators respectively. An EDP signal corresponding to exclusive dijet events produced via an exchange of two gluons at the lowest order of QCD [3] was generated using FPMC.

The data used in this analysis were collected with the $D\bar{O}$ detector in the period between August 2002 and April 2006 at the Tevatron Collider at a center-of-mass energy $\sqrt{s} = 1.96 \text{ TeV}$. The $D\bar{O}$ detector is described in detail elsewhere [11]. For this analysis, the most relevant components are the central and forward calorimeters used for jet reconstruction and the identification of a rapidity gap devoid of any energy (above noise) in the calorimeter. The $D\bar{O}$ liquid-argon and uranium calorimeter is divided in three parts housed in independent cryostats covering respectively the following regions in pseudo-rapidity: $|\eta| < 1.1$ (central calorimeter), and $1.6 < |\eta| < 4.2$ (two end cap calorimeters) where $\eta = -\ln[\tan(\frac{\theta}{2})]$ and θ is the polar angle. Jets in EDP events are expected to be more central than other jet production, therefore both jets are required to be central with a rapidity $|y| < 0.8$ where the rapidity is defined as $y = 0.5 \ln(E + p_z)/(E - p_z)$ where E and p_z are respectively the jet energy and the momentum along the beam axis. The forward region of the calorimeter is used to check the presence of a region devoid of any energy (above noise) on

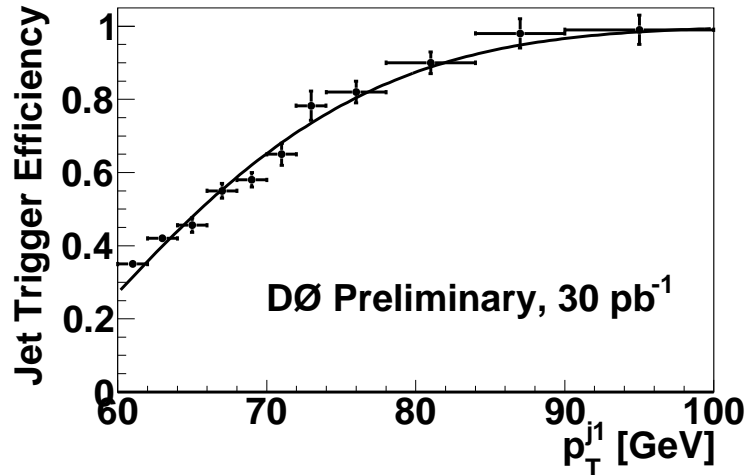


FIG. 2: 45 GeV jet trigger efficiency as a function of the leading jet p_T (p_T^{j1}). For events with $p_T^{j1} > 100$ GeV, the efficiency is 100% and no correction is needed.

each side of the dijet system.

Data were collected using a D0 inclusive jet trigger requiring at least one jet to be above a p_T threshold of 45 GeV. This choice is motivated to select exclusive diffractive events in the region of dijet invariant mass above 100 GeV. In addition, low $p\bar{p}$ interaction multiplicity events were selected to avoid the contamination of the rapidity gaps due to additional interactions in a given bunch crossing. The instantaneous luminosity used in the analysis was thus constrained to be in the range of $[5 - 100] \times 10^{30} \text{ cm}^{-2} \text{ s}^{-1}$, where the fraction of events with two or more $p\bar{p}$ interactions is less than 20%. Due to prescales imposed to avoid saturating the data acquisition system, the final luminosity of the sample is about 30 pb^{-1} . By comparing the jet p_T spectrum with data collected with a trigger with a lower p_T threshold of 15 GeV, the trigger was found not to be fully efficient for jet p_T between 60 and 100 GeV and the Monte Carlo events were reweighted with the trigger efficiency in this jet p_T range. The correction factors due to the trigger inefficiency as a function of jet p_T are given in Fig. 2.

Jets are reconstructed using an iterative midpoint cone algorithm [12] with a cone size $R = 0.7$. Since high p_T exclusive dijet events are mainly produced centrally, two central reconstructed jets with $|y| < 0.8$ are required. The highest- p_T (leading) and second-highest p_T jets are required to have p_T greater than 60 and 40 GeV respectively and only dijet events with an invariant mass greater than 100 GeV are selected for studies. In order to enhance the number of events without additional QCD radiation [3], which is expected for exclusive production, the two jets are required to be back-to-back in azimuthal angle φ , with a separation $\Delta\varphi > 3.1$ rad. An additional cosmic ray suppression is performed requiring that the missing transverse energy is less than 70% of the leading jet transverse energy.

The MC events are required to satisfy the same selection criteria as in data. They are processed through a GEANT-based [13] simulation of the D0 detector response and use the same reconstruction code as for data. They are weighted in order to take into account the trigger inefficiencies for jet p_T in the region 60-100 GeV. Data events from random $p\bar{p}$ crossings are overlaid on the MC events, using data from the same time period as considered in the analysis. The MC events are weighted in addition to obtain the same instantaneous luminosity profile as the data to obtain the same noises and extra energies in the forward region of the calorimeter in data. The sum of NDF, SD and IDP, each one weighted by their cross section, is normalised to data — the EDP contribution is negligible at this stage. Fig 3 shows the good agreement between the MC simulation and data after this rescaling. By varying the cut on the leading jet p_T , the uncertainty on the normalisation was estimated to be 5%.

It is possible to discriminate between exclusive events and background (NDF, SD and IDP) since a large rapidity gap is expected between the central jets and the proton and antiproton since no Pomeron or proton remnants are expected in EDP. Two different regions of pseudorapidity η are defined in the calorimeter far from the two central jets. The very forward region ($|\eta| > 3.0$) allows discrimination of diffractive events (SD and IDP) from NDF since proton remnants are present in this region of the calorimeter in NDF. The intermediate forward region ($2.0 < |\eta| < 3.0$) is used to identify EDP events since they show larger rapidity gaps than SD and IDP. To define a calorimeter region devoid of activity, noisy cells in the forward region of the calorimeters, which present an occupancy that differed by more than 5 standard deviations from the average, are removed. The cell response in MC was in addition adjusted to data by applying a MC-to-data correction factor for each cell using low jet p_T and minimum bias trigger data. After performing these corrections, the calorimeter cell information was used to form the Δ variable in order to discriminate

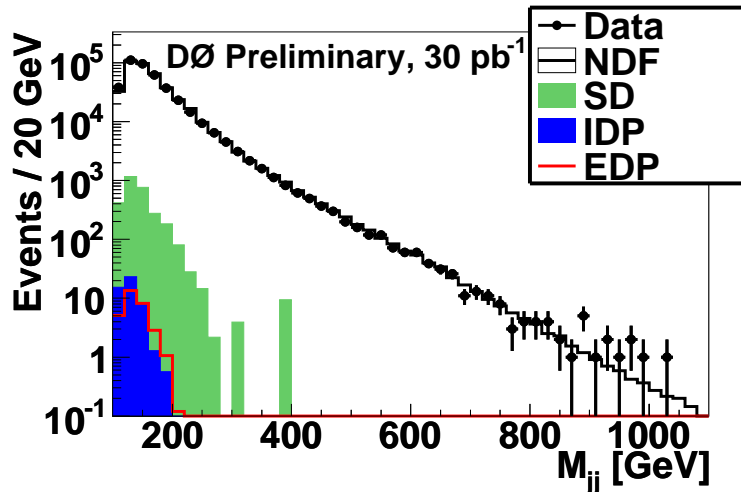


FIG. 3: Dijet invariant mass distribution for MC and data. A good agreement between the MC simulation and data is found after applying jet energy scale corrections and the different scale factors corresponding to the trigger efficiencies, the luminosity profiles, and the MC normalisation fitted to data.

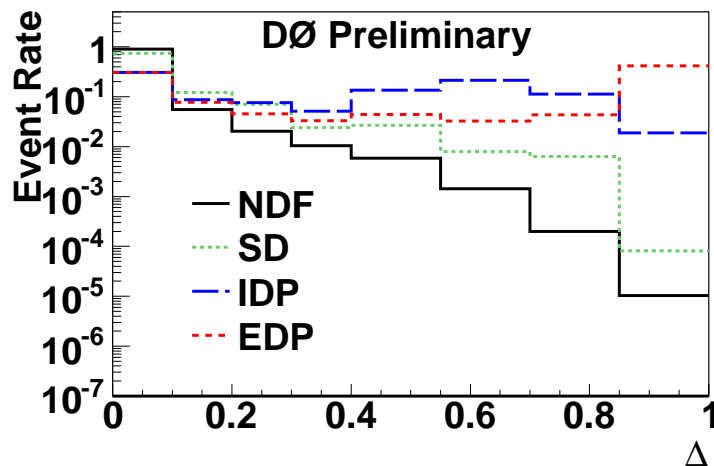


FIG. 4: Δ distribution normalised to unity for all MC samples. EDP peaks at $\Delta > 0.85$. The EDP at low Δ values is due to pile-up events, where a second proton-antiproton inelastic scattering occurs in the same bunch crossing.

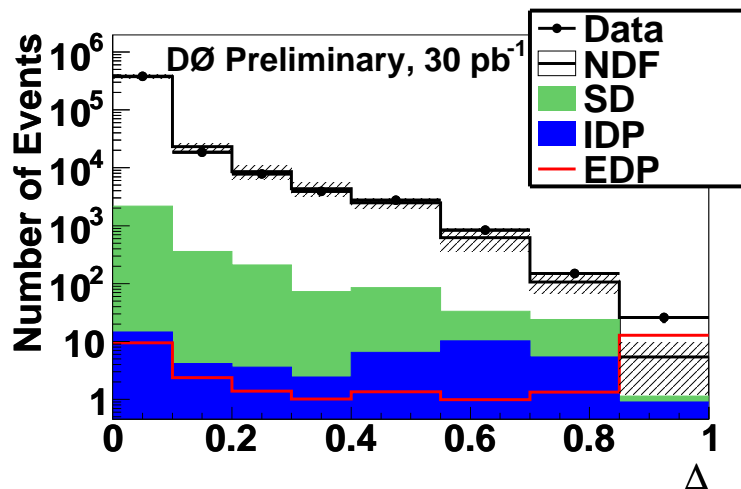
between the different classes of events

$$\Delta = \frac{1}{2} \exp\left(-\sum_{2.0 < |\eta| \leq 3.0} E_T / \text{GeV}\right) + \frac{1}{2} \exp\left(-\sum_{3.0 < |\eta| < 4.2} E_T / \text{GeV}\right). \quad (1)$$

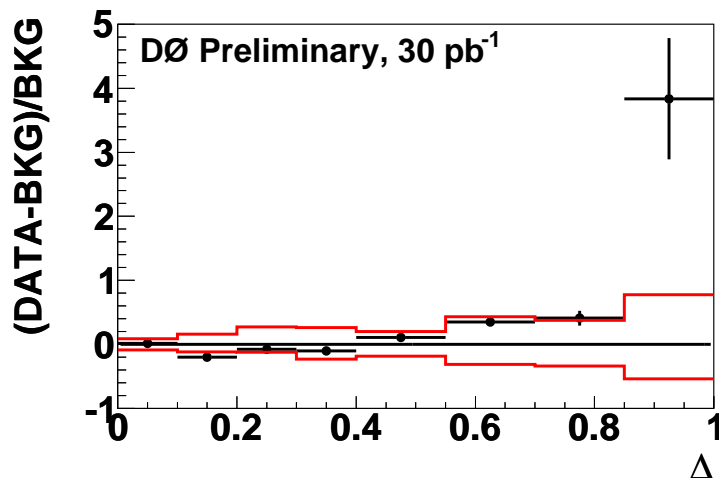
Here the sum is performed on the transverse energy (E_T) of all calorimeter cells within the considered regions. Fig. 4 displays Δ normalised to unity for all MC samples, including the expected EDP events peaking at $\Delta > 0.85$.

The leading systematic error is due to the uncertainty on the cell calibration factors. They are varied by three standard deviations from their central value leading to a change of 25% of the background for $\Delta > 0.85$. The effect of the jet energy scale uncertainties modifies the background by 12%. To estimate the systematic uncertainties due the trigger efficiency and instantaneous luminosity reweighting procedure, the analysis was redone using the 15 GeV jet p_T trigger threshold which lead to a 3% systematic uncertainty. As previously mentioned, an additional systematic uncertainty due to the MC to data normalisation is estimated to be 5%. An additional uncertainty of 50% on the SD and IDP MC normalisations was added.

Fig. 5 displays the comparison of the Δ distributions in data and MC (NDF, SD and IDP) normalised to their leading order cross sections. A good agreement is observed between data and MC except at high values of Δ where



(a)



(b)

FIG. 5: (a) Δ distribution for data and MC (NDF, SD and IDP). A good agreement is observed between data and MC except at high values of Δ where EDP dominates. The hatched band indicates the total uncertainty on the background. (b) MC background (BKG) subtracted data divided by background. The solid lines are ± 1 standard deviation systematic uncertainty on the background.

EDP dominates. The significance of the excess with respect to the NDF, SD and IDP backgrounds is determined using a modified frequentist method [14]. It is obtained via fits of the signal and background hypotheses to pseudo-data samples containing only background. The effect of systematic uncertainties are constrained by maximizing a likelihood function for signal and signal+background hypotheses over all systematic uncertainties and the pseudo experiments include fluctuations over each systematic uncertainty. The observed significance corresponds to the fraction of outcomes that yield an EDP cross section at least as large as that measured in data. Seven bins are used as input for the significance calculation: six bins for Δ between 0.1 and 0.85, where the bin used for the MC normalisation is removed; and the high $\Delta \geq 0.85$ bin. The probability for the observed excess to be explained by an upward fluctuation of the background is of 2×10^{-5} , corresponding to an excess of 4.1 standard deviations (the expected excess is of 2.8 standard deviations). Table I gives the observed number of events in data compared to background and EDP expectations. Fig. 6 displays the dijet invariant mass distribution for $\Delta > 0.85$. To illustrate the differences between the diffractive dijet exclusive event with $\Delta > 0.85$, where the calorimeter has little energy deposition outside the central region, and the non diffractive events, two event displays are shown in Fig. 7.

To summarize, we have presented evidence at the 4.1 standard deviation level for exclusive dijet production in $p\bar{p}$ collisions at a center-of-mass energy $\sqrt{s} = 1.96$ TeV with the D0 detector at high dijet invariant mass ($M_{JJ} > 100$ GeV). Such event signatures are expected to play an important role in future studies at the Tevatron and LHC.

Sample	NDF	IDP	SD	EDP	Data
No Δ cut	409527 ± 24056	48.3 ± 24.3	2930 ± 1474	30.9 ± 1.8	412505
$\Delta \geq 0.85$	4.2 ± 1.6	0.9 ± 0.4	0.2 ± 0.2	12 ± 0.9	26

TABLE I: Number of predicted events for each MC sample before and after the cut on Δ . The statistic and systematic uncertainties are added in quadrature.

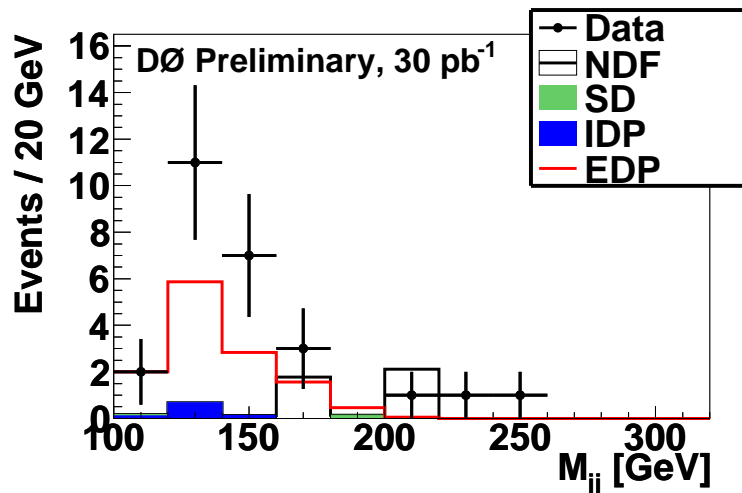


FIG. 6: Dijet invariant mass distribution for MC and data after applying the cut on $\Delta \geq 0.85$. The total background prediction is of $5.4^{+4.2}_{-2.9}$ events and 26 signal candidate events are observed in data.

We thank the staffs at Fermilab and collaborating institutions, and acknowledge support from the DOE and NSF (USA); CEA and CNRS/IN2P3 (France); FASI, Rosatom and RFBR (Russia); CNPq, FAPERJ, FAPESP and FUNDUNESP (Brazil); DAE and DST (India); Colciencias (Colombia); CONACyT (Mexico); KRF and KOSEF (Korea); CONICET and UBACyT (Argentina); FOM (The Netherlands); STFC and the Royal Society (United Kingdom); MSMT and GACR (Czech Republic); CRC Program and NSERC (Canada); BMBF and DFG (Germany); SFI (Ireland); The Swedish Research Council (Sweden); and CAS and CNSF (China).

-
- [1] G. Ingelman and P. E. Schlein, Phys. Lett. B **152**, 256 (1985). M. Boonekamp, F. Chevallier, C. Royon and L. Schoeffel, Acta Phys. Polon. B **40**, 2239 (2009).
- [2] B. Abbott *et al.* (D0 Collaboration), Phys. Lett. B **531**, 52 (2002).
- [3] V. A. Khoze, A. D. Martin and M. G. Ryskin, Eur. Phys. J. C **14**, 525 (2000) [arXiv:hep-ph/0002072]; V. A. Khoze, A. D. Martin and M. G. Ryskin, Eur. Phys. J. C **19**, 477 (2001) [Erratum-ibid. C **20**, 599 (2001)] [arXiv:hep-ph/0011393].
- [4] M. Boonekamp, R. B. Peschanski and C. Royon, Phys. Lett. B **598**, 243 (2004). C. Royon [RP220 Collaboration], arXiv:0706.1796 [physics.ins-det]. M. G. Albrow *et al.* [FP420 R&D Collaboration], arXiv:0806.0302 [hep-ex].
- [5] T. Aaltonen *et al.* [CDF Collaboration], Phys. Rev. D **77**, 052004 (2008). T. Aaltonen *et al.* [CDF Collaboration], Phys. Rev. Lett. **99**, 242002 (2007). T. Aaltonen *et al.* [CDF Collaboration], Phys. Rev. Lett. **102**, 222002 (2009). T. Aaltonen *et al.* [CDF Collaboration], Phys. Rev. Lett. **102**, 242001 (2009). A. Abulencia *et al.* [CDF Collaboration], Phys. Rev. Lett. **98**, 112001 (2007).
- [6] A. Aktas *et al.* [H1 Collaboration], Eur. Phys. J. C **48**, 715 (2006).
- [7] V. A. Khoze, A. D. Martin and M. G. Ryskin, Eur. Phys. J. C **23**, 311 (2002); E. Gotsman, E. Levin, U. Maor, E. Naftali and A. Prygarin, arXiv:hep-ph/0511060; A. Kupco, C. Royon, R. Peschanski, Phys. Lett. B **606**, 139 (2005).
- [8] T. Sjöstrand *et al.*, Comput. Phys. Commun. **135**, 238 (2001).
- [9] B. E. Cox and J. R. Forshaw, Comput. Phys. Commun. **144**, 104 (2002) [arXiv:hep-ph/0010303].
- [10] M. Boonekamp, V. Juranek, O. Kepka, C. Royon, Proceedings of the Workshop of the Implications of HERA for LHC physics, DESY-Proc-2009-02.
- [11] V.M. Abazov *et al.* (D0 Collaboration), Nucl. Instrum. Methods Phys. Res. A **565**, 463 (2006).
- [12] G.C. Blazey *et al.*, in *Proceedings of the Workshop: QCD and Weak Boson Physics in Run II*, edited by U. Baur, R.K. Ellis,

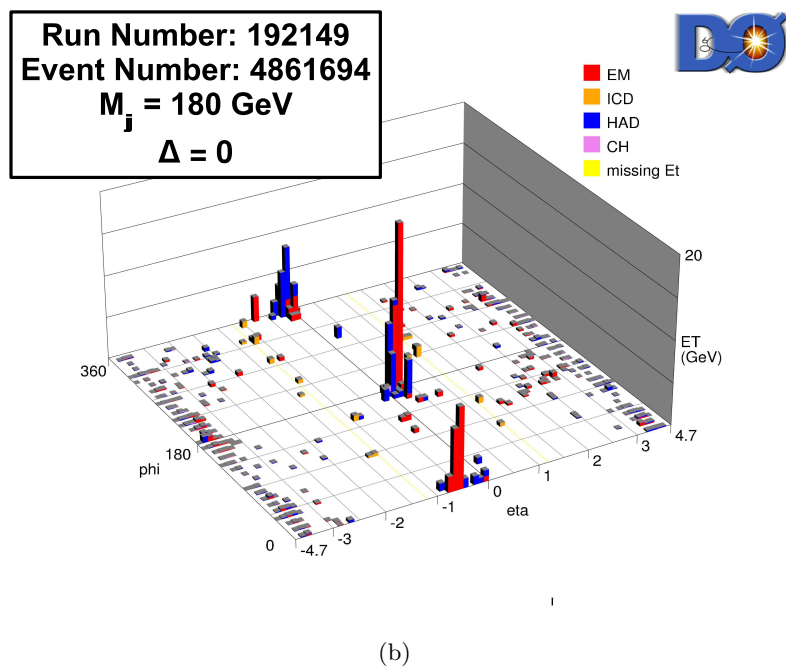
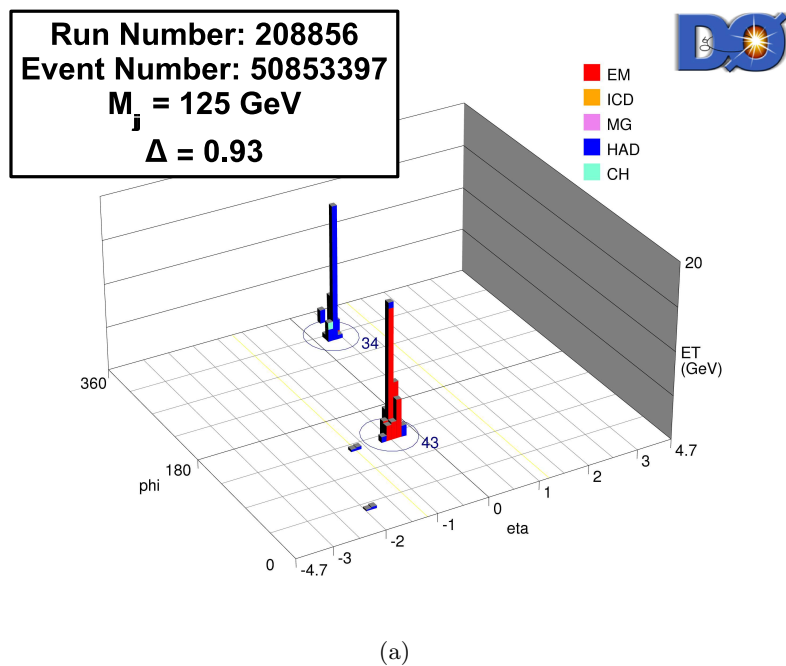


FIG. 7: D0 event displays: (a) Exclusive diffractive event. No energy deposition is present in the forward regions, only two central jets are observed in the detector. (b) Background event. In addition to the two jets present in the detector, energy deposition is present in the forward regions.

and D. Zeppenfeld, Fermilab-Pub-00/297 (2000).

[13] R. Brun and F. Carminati, CERN Program Library Long Writeup W5013, 1993 (unpublished).

[14] W. Fisher, FERMILAB-TM-2386-E (2006).